Alkyl and Aryl Substituted Corroles. 2. Synthesis and Characterization of Linked "Face-to-Face" Biscorroles. X-ray Structure of $(BCA)Co_2(py)_3$, Where BCA Represents a Biscorrole with an Anthracenyl Bridge

Roger Guilard,*,† François Jérôme,† Jean-Michel Barbe,† Claude P. Gros,† Zhongping Ou,‡ Jianguo Shao,‡ Jean Fischer,§ Raymond Weiss,*,§ and Karl M. Kadish*,‡

LIMSAG UMR 5633, Faculté des Sciences Gabriel, Université de Bourgogne, 6, Boulevard Gabriel, 21000 Dijon, France, Department of Chemistry, University of Houston, Houston, Texas 77204-5641, and Institut Le Bel, Université Louis Pasteur, 4, Rue Blaise Pascal, 67000 Strasbourg, France

Received February 9, 2001

The synthesis, spectroscopic properties, and electrochemistry of $(BCA)Co_2$ and $(BCB)Co_2$ are described where BCA and BCB represent biscorroles linked by an anthracenyl (A) or a biphenylenyl (B) bridge. The pyridine and CO binding properties of $(BCA)Co_2$ and $(BCB)Co_2$ are also presented, and one of the compounds in its pyridine-ligated form, $(BCA)Co_2(py)_3$, is structurally characterized. The data on the biscorroles are compared on one hand to the monocorrole having the same substitution pattern and on the other hand to bisporphyrins having two Co(II) ions and the same anthracenyl or biphenylenyl linkers in order to better understand the interaction which occurs between the two corrole macrocycles. A parallel study on five different Co(III) phenyl-substituted corroles showed that bis-pyridine and mono-CO adducts are readily formed from the complexes in CH_2Cl_2. This present paper examines how the ligand binding properties and electrochemistry of these Co(III) corroles are modified by the anthracenyl or biphenylenyl bridge which links the two macrocycles in a face to face orientation. An X-ray crystal structure was obtained for the tris-pyridine adduct of the anthracenyl bridged derivative, $(BCA)Co_2(py)_3$, and gives the following results: $C_{127}H_{99}Co_2N_{11}\cdot 2CHCl_3$, $M = 2135.90$, triclinic, space group $P\bar{1}$, $a = 13.2555(5)$ Å, $b = 18.6406(8)$ Å, $c = 22.2140(9)$ Å, $\alpha = 94.186(9)°$, $\beta = 102.273(9)°$, $\gamma = 94.205(9)°$, $V = 5326.8(4)$ Å^3, 9293 independent reflections collected, $R(F) = 0.066$.

Introduction

Model cofacial bisporphyrins can generally be grouped into two types of compounds, those linked on opposite sides of each macrocycle with two flexible strapping units[1−7] and those linked on only one side of each macrocycle by a rigid linking unit.[8−19] Among these latter derivatives are the cofacial bisporphyrin systems with anthracenyl or biphenylenyl spacers, the so-called "Pacman" porphyrin systems $(DPA)H_4$ and $(DPB)H_4$, where DPA and DPB represent bisporphyrins with anthracenyl (A) or biphenylenyl (B) bridges.[8−15,20,21]

The great importance assumed by bisporphyrins in oxygen activation[9,22−28] and the parallel development of corrole

† Université de Bourgogne.
‡ University of Houston.
§ Université Louis Pasteur.

(1) Collman, J. P.; Anson, F. C.; Barnes, C. E.; Bencosme, C. S.; Geiger, T.; Evitt, E. R.; Kreh, R. P.; Meier, K.; Pettman, R. B. *J. Am. Chem. Soc.* **1983**, *105*, 2694−2699.
(2) Kim, K. Ph.D. dissertation, Stanford University, 1987.
(3) Collman, J. P.; Bencosme, C. S.; Barnes, C. E.; Miller, B. D. *J. Am. Chem. Soc.* **1983**, *105*, 2704−2710.
(4) Collman, J. P.; Denisevich, P.; Konai, Y.; Marrocco, M.; Koval, K.; Anson, F. C. *J. Am. Chem. Soc.* **1980**, *102*, 6027−6036.
(5) Hatada, M. H.; Tulinsky, A.; Chang, C. K. *J. Am. Chem. Soc.* **1980**, *102*, 7115−7116.
(6) Collman, J. P.; Chong, A. O.; Jamieson, G. B.; Oakley, R. T.; Rose, E.; Schmittou, E. R.; Ibers, J. A. *J. Am. Chem. Soc.* **1981**, *103*, 516−533.
(7) Lindsey, J. S. In *The Porphyrin Handbook*; Kadish, K. M., Smith, K. M., Guilard, R., Eds.; Academic Press: San Diego, CA, 2000; Vol. 1, pp 45−118.
(8) Collman, J. P.; Hutchison, J. E.; Lopez, M. A.; Tabard, A.; Guilard, R.; Seok, W. K.; Ibers, J. A.; L'Her, M. *J. Am. Chem. Soc.* **1992**, *114*, 9869−9877.
(9) Barbe, J.-M.; Guilard, R. In *The Porphyrin Handbook*; Kadish, K. M., Smith, K. M., Guilard, R., Eds.; Academic Press: San Diego, CA, 2000; Vol. 3, pp 211−244.
(10) Collman, J. P.; Hutchison, J. E.; Lopez, M. A.; Guilard, R. *J. Am. Chem. Soc.* **1992**, *114*, 8066−8073.
(11) Chang, C. K.; Abdalmuhdi, I. *J. Org. Chem.* **1983**, *48*, 5388−5390.
(12) Chang, C. K.; Abdalmuhdi, I. *Angew. Chem., Int. Ed. Engl.* **1984**, *23*, 164−165.
(13) Guilard, R.; Lopez, M. A.; Tabard, A.; Richard, P.; Lecomte, C.; Brandès, S.; Hutchison, J. E.; Collman, J. P. *J. Am. Chem. Soc.* **1992**, *114*, 9877−9889.
(14) Guilard, R.; Brandès, S.; Tabard, A.; Bouhmaida, N.; Lecomte, C.; Richard, P.; Latour, J. M. *J. Am. Chem. Soc.* **1994**, *116*, 10202−10211.
(15) Guilard, R.; Brandès, S.; Tardieux, C.; Tabard, A.; L'Her, M.; Miry, C.; Gouerec, P.; Knop, Y.; Collman, J. P. *J. Am. Chem. Soc.* **1995**, *117*, 11721−11729.
(16) Sessler, J. L.; Johnson, M. R.; Creager, S. E.; Fettinger, J. C.; Ibers, J. A. *J. Am. Chem. Soc.* **1990**, *112*, 9310−9329.
(17) Fillers, J. P.; Ravichandran, K. G.; Abdalmuhdi, I.; Tulinsky, A.; Chang, C. K. *J. Am. Chem. Soc.* **1986**, *108*, 417−424.
(18) Chang, C. J.; Deng, Y.; Heyduk, A. F.; Chang, C. K.; Nocera, D. G. *Inorg. Chem.* **2000**, *39*, 959−966.
(19) Deng, Y.; Chang, C. J.; Nocera, D. G. *J. Am. Chem. Soc.* **2000**, *122*, 410−411.
(20) Collman, J. P.; Hutchison, J. E.; Lopez, M. A.; Guilard, R.; Reed, R. A. *J. Am. Chem. Soc.* **1991**, *113*, 2794−2796.
(21) Brandès, S. Ph.D. dissertation, Université de Bourgogne, 1993.
(22) Chang, C. K.; Liu, H.-Y.; Abdalmuhdi, I. *J. Am. Chem. Soc.* **1984**, *106*, 2725−2726.
(23) Chang, C. J.; Deng, Y.; Shi, C.; Chang, C. K.; Anson, F. C.; Nocera, D. G. *Chem. Commun.* **2000**, 1355−1356.
(24) Collman, J. P.; Elliot, C. M.; Halbert, T. R.; Tovrog, B. S. *Proc. Natl. Acad. Sci. U.S.A.* **1977**, *74*, 18−22.
(25) Hutchison, J. E.; Postlethwaite, T. A.; Chen, C. H.; Hathcock, K. W.; Ingram, R. S.; Ou, W.; Linton, R. W.; Murray, R. W.; Tyvoll, D. A.; Chng, L. L.; Collman, J. P. *Langmuir* **1997**, *13*, 2143-2148.

10.1021/ic0101782 CCC: $20.00 © 2001 American Chemical Society
Published on Web 08/17/2001

Chart 1

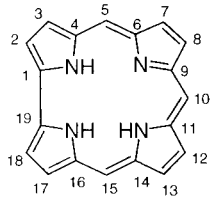

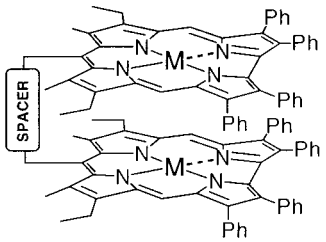

(BCA)M_2 : spacer = anthracenyl bridge (**a**)
7a : M = 3H
8a : M = Co

(BCB)M_2 : spacer = biphenylenyl bridge (**b**)
7b : M = 3H
8b : M = Co

chemistry[29−47] have provided a stimulation to synthesize corrole dyads with transition metals.[30,48,49] Indeed, corroles can be considered as intermediates between corrins and porphyrins since they present a direct link between two pyrroles and retain an 18 π-electron aromatic system.

Recently, we reported, in a preliminary communication, the first synthesis of sterically hindered cofacial biscorroles (BCA)H_6 and (BCB)H_6, where BCA and BCB represent biscorroles with anthracenyl (A) or biphenylenyl (B) bridges.[48,49] We now report the full synthesis and spectroscopic properties of these face-to-face biscorroles, which are shown in Chart 1. The ligand binding and electrochemical properties of (BCB)Co_2, **8b**, and (BCA)Co_2, **8a**, are also presented, and one of the compounds in its pyridine-ligated form, (BCA)$Co_2(py)_3$, is structurally characterized. These data are then compared to a related monocorrole having the same substitution pattern in order to better understand the interaction between the two sets of macrocycles. A parallel study on five different Co(III) phenyl-substituted corroles shows that bis-pyridine and mono-CO adducts are readily formed in CH_2Cl_2.[50] This present paper examines how ligand binding properties for a specific Co(III) corrole are modified by the anthracenyl or biphenylenyl bridge which links the two macrocycles in a face to face orientation.

Experimental Section

Instrumentation. ^{1}H NMR spectra were recorded on a Bruker AC 200 Fourier transform spectrometer at the Centre de Spectrométrie Moléculaire de l'Université de Bourgogne; chemical shifts are expressed in parts per million relative to chloroform (7.258 ppm). Microanalyses were performed at the Université de Bourgogne on a Fisons EA 1108 CHNS instrument. UV−visible spectra were recorded on a Varian Cary 1 spectrophotometer. Mass spectra were obtained with a Kratos Concept 32 S spectrometer in EI or LSIMS (*m*-NBA as matrix) modes. Cyclic voltammetry was carried out with an EG&G model 173 potentiostat. A three-electrode system was used and consisted of a glassy carbon or platinum disk working electrode, a platinum wire counter electrode, and a saturated calomel reference electrode (SCE). The SCE was separated from the bulk of the solution by a fritted-glass bridge of low porosity which contained the solvent/supporting electrolyte mixture. All potentials are referenced to the SCE.

UV−visible spectroelectrochemical experiments were performed with an optically transparent platinum thin-layer electrode of the type described in the literature.[51] Potentials were applied with an EG&G model 173 potentiostat. Time-resolved UV−visible spectra were recorded with a Hewlett-Packard model 8453 diode array rapid-scanning spectrophotometer. Infrared spectra were recorded on an FTIR Nicolet

(26) Le Mest, Y.; L'Her, M.; Saillard, J. Y. *Inorg. Chim. Acta* **1996**, *248*, 181−191.
(27) Le Mest, Y.; Inisan, C.; Laouenan, A.; L'Her, M.; Talarmin, J.; El Kalifa, M.; Saillard, J.-Y. *J. Am. Chem. Soc.* **1997**, *119*, 6095−6106.
(28) Liu, H.-Y.; Abdalmuhdi, I.; Chang, C. K.; Anson, F. C. *J. Phys. Chem.* **1985**, *89*, 665−670.
(29) Erben, C.; Will, S.; Kadish, K. M. In *The Porphyrin Handbook*; Kadish, K. M., Smith, K. M., and Guilard, R., Eds.; Academic Press: San Diego, CA, 2000; Vol. 2, pp 233−300.
(30) Paolesse, R. In *The Porphyrin Handbook*; Kadish, K. M., Smith, K. M., and Guilard, R., Eds.; Academic Press: San Diego, CA, 2000; Vol. 2, pp 201−232.
(31) Kadish, K. M.; Will, S.; Adamian, V. A.; Walther, B.; Erben, C.; Ou, Z.; Guo, N.; Vogel, E. *Inorg. Chem.* **1998**, *37*, 4573−4577.
(32) Kadish, K. M.; Adamian, V. A.; Van Caemelbecke, E.; Gueletii, E.; Will, S.; Erben, C.; Vogel, E. *J. Am. Chem. Soc.* **1998**, *120*, 11986−11993.
(33) Autret, M.; Will, S.; Van Caemelbecke, E.; Lex, J.; Gisselbrecht, J.-P.; Gross, M.; Vogel, E.; Kadish, K. M. *J. Am. Chem. Soc.* **1994**, *116*, 9141−9149.
(34) Van Caemelbecke, E.; Will, S.; Autret, M.; Adamian, V. A.; Lex, J.; Gisselbrecht, J.-P.; Gross, M.; Vogel, E.; Kadish, K. M. *Inorg. Chem.* **1996**, *35*, 184−192.
(35) Adamian, V. A.; D'Souza, F.; Licoccia, S.; Di Vona, M. L.; Tassoni, E.; Paolesse, R.; Boschi, T.; Kadish, K. M. *Inorg. Chem.* **1995**, *34*, 532−540.
(36) Kadish, K. M.; Lin, X. Q.; Han, B. C. *Inorg. Chem.* **1987**, *26*, 4161−4167.
(37) Kadish, K. M.; Koh, W.; Tagliatesta, P.; Sazou, D.; Paolesse, R.; Licoccia, S.; Boschi, T. *Inorg. Chem.* **1992**, *31*, 2305−2313.
(38) Will, S.; Lex, J.; Vogel, E.; Adamian, V. A.; Van Caemelbecke, E.; Kadish, K. M. *Inorg. Chem.* **1996**, *35*, 5577−5583.
(39) Kadish, K. M.; Erben, C.; Ou, Z.; Adamian, V. A.; Will, S.; Vogel, E. *Inorg. Chem.* **2000**, *39*, 3312−3319.
(40) Cho, W.-S.; Lee, C.-H. *Tetrahedron Lett.* **2000**, *41*, 697−701.
(41) Ghosh, A.; Wondimagegn, T.; Parusel, A. B. J. *J. Am. Chem. Soc.* **2000**, *122*, 5100−5104.
(42) Gross, Z.; Simkhovich, L.; Galili, N. *Chem. Commun.* **1999**, 599−600.
(43) Gross, Z.; Galili, N.; Saltsman, I. *Angew. Chem., Int. Ed. Engl.* **1999**, *38*, 1427−1429.
(44) Gross, Z.; Galili, N. *Angew. Chem., Int. Ed. Engl.* **1999**, *38*, 2366−2369.
(45) Gross, Z.; Galili, N.; Simkhovich, L.; Saltsman, I.; Botoshansky, M.; Bläser, D.; Boese, R.; Goldberg, I. *Org. Lett.* **1999**, *1*, 599−602.
(46) Simkhovich, L.; Goldberg, I.; Gross, Z. *J. Inorg. Biochem.* **2000**, *80*, 235−238.
(47) Simkhovich, L.; Galili, J.; Saltsman, I.; Goldberg, I.; Gross, Z. *Inorg. Chem.* **2000**, *39*, 2704−2705.
(48) Jérôme, F.; Gros, C. P.; Tardieux, C.; Barbe, J.-M.; Guilard, R. *Chem. Commun.* **1998**, 2007−2008.
(49) Guilard, R.; Jérôme, F.; Gros, C. P.; Barbe, J. M.; Ou, Z.; Shao, J.; Kadish, K. M. *C. R. Acad. Sci., Sér. 2* **2001**, 245−254.
(50) Guilard, R.; Gros, C. P.; Bolze, F.; Jérôme, F.; Ou, Z.; Shao, J.; Fischer, J.; Weiss, R.; Kadish, K. M. *Inorg. Chem.* **2001**, *40*, 4845−4855.
(51) Lin, X. Q.; Kadish, K. M. *Anal. Chem.* **1985**, *57*, 1498−1501.

Magna-IR 550 spectrometer. The background was obtained by recording the IR spectrum of CH_2Cl_2 saturated with CO and the IR spectrum of the compound under CO was obtained after bubbling CO through the solution for 10−15 min.

Chemicals and Reagents. Absolute dichloromethane (CH_2Cl_2) and pyridine (py) were obtained from Fluka Chemical Co. and used as received. Tetra-*n*-butylammonium perchlorate (TBAP, Fluka Chemical Co.) was twice recrystallized from absolute ethanol and dried in a vacuum oven at 40 °C for a week. Compounds **1a**, **1b**, **2**, and **5** were synthesized as described elsewhere.[21,48]

1,8-Bis(5,5′-ethoxycarbonyl-4,4′-diethyl-3,3′-dimethyldipyrromethan-5-yl)anthracene (3a). A mixture of 1 g of 1,8-diformylanthracene (**1a**) (4.3 mmol) and 3.25 g of 5-ethoxycarbonyl-4-ethyl-3-methylpyrrole (**2**) (18 mmol) was dissolved in 60 mL of hot ethanol. A 3 mL aliquot of concentrated hydrochloric acid were then added, and the mixture was stirred under reflux for 5 h. The reaction medium was cooled to room temperature, and the resulting solid was filtered and washed by cold methanol and then dried to give the title product **3a** (3.35 g, 85%). ^{1}H NMR: δ 8.49 (s, 4H), 8.48 (s, 1H), 8.32 (s, 1H), 7.95 (d, 2H, $^3J_{H-H}$ = 8.0 Hz), 7.33 (dd, 2H, $^3J_{H-H}$ = 8.0 Hz), 6.92 (d, 2H, $^3J_{H-H}$ = 8.0 Hz), 5.85 (s, 2H), 4.19 (q, 8H, $^3J_{H-H}$ = 6.0 Hz), 3.68 (q, 8H, $^3J_{H-H}$ = 8.0 Hz), 1.60 (s, 12H), 1.24 (t, 12H, $^3J_{H-H}$ = 8.0 Hz), 1.05 (t, 12H, $^3J_{H-H}$ = 8.0 Hz). MS: m/z = 922 $[M]^{\bullet+}$. Anal. Calcd for $C_{56}H_{66}N_4O_8$: C, 72.86; H, 7.21; N, 6.07. Found: C, 72.76; H, 7.29; N, 5.99.

1,6-Bis(5,5′-ethoxycarbonyl-4,4′-diethyl-3,3′-dimethyldipyrromethan-5-yl)biphenylene (3b). This compound was prepared in 89% yield (3.83 g), as described above for **3a**, starting from **1b** (1 g, 4.8 mmol) and **2** (3.25 g, 20 mmol). ^{1}H NMR: δ 8.24 (s, 4H), 6.92 (d, 2H, $^3J_{H-H}$ = 8.0 Hz), 6.71 (dd, 2H, $^3J_{H-H}$ = 8.0 Hz), 6.61 (d, 2H, $^3J_{H-H}$ = 8.0 Hz), 5.28 (s, 2H), 4.24 (q, 8H, $^3J_{H-H}$ = 6.0 Hz), 2.68 (q, 8H, $^3J_{H-H}$ = 6.0 Hz), 2.16 (s, 12H), 1.33 (t, 12H, $^3J_{H-H}$ = 6.0 Hz), 1.01 (t, 12H, $^3J_{H-H}$ = 6.0 Hz). MS: m/z = 897 $[M]^{\bullet+}$. Anal. Calcd for $C_{54}H_{64}N_4O_8$: C, 72.30; H, 7.19; N, 6.25. Found: C, 72.41; H, 7.15; N, 6.09.

1,8-Bis(4,4′-diethyl-3,3′-dimethyldipyrromethan-5-yl)anthracene (4a). A suspension of 2.86 g of **3a** (3 mmol) in diethylene glycol (150 mL) containing KOH (15 g) was heated at 190 °C under N_2 for 3 h and then allowed to cool to room temperature. The mixture was poured into ice water (500 mL), and the resulting solid was filtered, washed with water, and then dried to give the title product **4a** (1.76 g, 90%). ^{1}H NMR: δ 8.68 (s, 1H), 8.44 (s, 1H), 7.88 (d, 2H, $^3J_{H-H}$ = 8.5 Hz), 7.32 (dd, 2H, $^3J_{H-H}$ = 8.5 Hz), 7.02 (d, 2H, $^3J_{H-H}$ = 8.5 Hz), 6.93 (s, 4H), 6.31 (d, 2H, $^3J_{H-H}$ = 2.5 Hz), 5.99 (s, 2H), 2.41 (q, 8H, $^3J_{H-H}$ = 7.3 Hz), 1.72 (s, 12H), 1.15 (t, 12H, $^3J_{H-H}$ = 7.3 Hz). MS: m/z = 634 $[M]^{\bullet+}$. Anal. Calcd for $C_{56}H_{66}N_4O_8$: C, 83.24; H, 7.94; N, 8.82. Found: C, 83.58; H, 7.71; N, 8.61.

1,6-Bis(4,4′-diethyl-3,3′-dimethyldipyrromethan-5-yl)biphenylene (4b). This compound was prepared in 92% yield (1.25 g), as described for **4a**, starting from **3b** (2 g, 2.2 mmol). ^{1}H NMR: δ 7.07 (s, 4H), 6.44 (m, 5H), 6.11 (d, 1H, $^3J_{H-H}$ = 2.4 Hz), 5.11 (s, 2H), 2.48 (q, 8H, $^3J_{H-H}$ = 7.3 Hz), 1.87 (s, 12H), 1.24 (t, 12H, $^3J_{H-H}$ = 7.3 Hz). MS: m/z = 608 $[M]^{\bullet+}$. Anal. Calcd for $C_{42}H_{48}N_4$: C, 82.85; H, 7.95; N, 9.20. Found: C, 82.76; H, 7.31; N, 9.68.

1,8-Bis(7,13-diethyl-8,12-dimethyl-2,3,17,18-tetraphenylcorrol-10-yl)anthracene (7a). A mixture of 0.55 g (0.86 mmol) of **4a** and 0.9 g (3.6 mmol) of 3,4-diphenyl-2-formylpyrrole **5** was dissolved in methanol (500 mL). HBr/CH_3CO_2H (2.2 mL) was then added, and the resulting mixture was stirred at room temperature for 4 h after which $NaHCO_3$ (2.2 g) was added and the mixture stirred again for 10 min. *p*-Chloranil (0.075 g) and hydrazine hydrate (3.5 mL) were then added and stirring continued for 20 min after which the solvent was evaporated under vacuum and the solid dissolved in CH_2Cl_2. The organic layer was washed with water, dried over $MgSO_4$, and evaporated. The solid was chromatographed on basic alumina (grade III, CH_2Cl_2 as eluent), and the first violet band was collected to give the title biscorrole **7a**. It was recrystallized from CH_2Cl_2/methanol (0.41 g, 23%). ^{1}H NMR: δ 8.86 (s, 4H), 8.79 (s, 1H), 8.36 (d, 2H, $^3J_{H-H}$ = 6.5 Hz), 7.98 (s, 1H), 7.80 (m, 8H, Ph), 7.65 (d, 2H, $^3J_{H-H}$ = 6.5 Hz), 7.57 (dd, 2H, $^3J_{H-H}$ = 6.5 Hz), 7.52 (m, 8H, Ph), 7.29 (m, 8H, Ph), 7.01 (m, 16H, Ph), 3.27 (dq, 4H, $^2J_{H-H}$ = 14.7 Hz, $^3J_{H-H}$ = 7.5 Hz), 3.22 (dq, 4H, $^2J_{H-H}$ = 14.7 Hz, $^3J_{H-H}$ = 7.5 Hz), 1.95 (s, 12H), 1.31 (t, 12H, $^3J_{H-H}$ = 7.5 Hz), −2.83 (s, 4H), −3.00 (s, 2H). MS: m/z = 1549 $[M + H]^+$. IR (KBr): ν 3482 (NH), 3401 (NH), 2961(CH), 2923 (CH), 2870 (CH) cm^{-1}. UV−vis (CH_2Cl_2; λ_{max}, nm (ϵ, L mol^{-1} cm^{-1})): 416 nm (131 500), 572 (35 400), 608 (29 000). Anal. Calcd for $C_{112}H_{90}N_8 \cdot 2H_2O$: C, 84.92; H, 5.98; N, 7.07. Found: C, 84.96; H, 6.00; N, 6.98.

1,6-Bis(7,13-diethyl-8,12-dimethyl-2,3,17,18-tetraphenylcorrol-10-yl)biphenylene (7b). This compound was prepared in 20% yield (0.25 g), as described for **7a**, starting from **4b** (0.5 g, 0.82 mol) and **5** (0.85 g, 3.4 mol). ^{1}H NMR: δ 9.59 (s, 4H), 7.98 (d, 2H, $^3J_{H-H}$ = 6.5 Hz), 7.61 (dd, 2H, $^3J_{H-H}$ = 6.5 Hz) 7.47 (d, 2H, $^3J_{H-H}$ = 6.5 Hz), 7.10 (m, 40H), 3.54 (m, 8H), 2.07 (s, 12H), 1.52 (t, 12H, $^3J_{H-H}$ = 7.3 Hz), −5.49 (s, 6H). MS: m/z = 1523 $[M + H]^+$. UV−vis (CH_2Cl_2; λ_{max}, nm (ϵ, L mol^{-1} cm^{-1})): 404 nm (141 000), 578 (44 500), 607 (37 000). Anal. Calcd for $C_{110}H_{88}N_8$: C, 86.81; H, 5.83; N, 7.36. Found: C, 86.64; H, 5.98; N, 7.45.

1,8-Bis[cobalt(III) 7,13-diethyl-8,12-dimethyl-2,3,17,18-tetraphenylcorrol-10-yl]anthracene (8a). Compound **7a** (0.2 g, 0.13 mmol) was added to a solution of cobalt(II) acetate (0.16 g, 0.65 mmol) in pyridine (20 mL). The solution was heated at 80 °C, and the reaction was monitored by UV−visible spectroscopy. The solvent was then evaporated under vacuum, and the residue was chromatographed on a Florisil column (CH_2Cl_2 + 1% methanol as eluent). The second red band afforded the title product (**8a**) which was recrystallized from CH_2Cl_2/methanol (82 mg, 41%). MS: m/z = 1660 $[M]^{\bullet+}$. UV−vis (CH_2Cl_2; λ_{max}, nm (ϵ, L mol^{-1} cm^{-1})): 402 nm (90 000), 527 (26 000). Anal. Calcd. for $C_{112}H_{84}N_8Co_2 \cdot CH_3OH$: C, 80.22; H, 5.24; N, 6.62. Found: C, 79.99; H, 5.21; N, 6.54.

1,6-Bis[cobalt(III) 7,13-diethyl-8,12-dimethyl-2,3,17,18-tetraphenylcorrol-10-yl]biphenylene (8b). This compound was obtained in 45% yield, as described for **8a**, starting from **7b** (0.2 g, 0.13 mmol). MS: m/z = 1634 $[M]^{\bullet+}$. UV−vis (CH_2Cl_2; λ_{max}, nm (ϵ, L mol^{-1} cm^{-1})): 390 nm (88 100), 521 (27 200). Anal. Calcd for $C_{110}H_{82}N_8Co_2.2CH_3OH$: C, 79.23; H, 5.34; N, 6.60. Found: C, 79.02; H, 5.41; N, 6.48.

Equilibrium Measurements. The binding of pyridine to (BCA)Co_2, **8a**, and (BCB)Co_2, **8b**, was carried out at 296 K in CH_2Cl_2 and the reaction monitored by UV−visible spectroscopy. The absorbance was fitted to the Hill equation[52]

$$\log((A_i - A_0)/(A_f - A_i)) = \log K + p \log [py] \qquad (1)$$

where A_i = absorbance at a specific concentration of pyridine; A_0 = initial absorbance where [py] = 0, and A_f = final absorbance where the fully ligated corrole is the only species present and p represents the number of ligands bound to cobalt center. Values for log K were obtained from the intercept of the line for a plot of $\log((A_i - A_0)/(A_f - A_i))$ vs log [py]. The concentration of the biscorroles for these measurements was 1×10^{-5} M, and that of pyridine was in the range of 10^{-5} to 0.5 M.

A calibrated gas tight syringe was used to introduce CO into CH_2Cl_2 solutions containing the examined corroles. The pressure of CO within the gas tight syringe ($P_{injected}$) was read from a barometer before each injection. The volume of the titration vessel above the solution (V_{vessel}) was 175 mL. Thus, by systematically injecting a known volume ($V_{injected}$) of CO gas into the vessel, we were able to calculate the partial pressure of CO (P^{CO}) at each step in the titration as $(V_{injected}/V_{vessel})$-$P_{injected}$. Each solution was vigorously shaken for 3 min after introducing CO to ensure equilibrium before recording the UV−visible spectrum. $P_{1/2}^{CO}$, the pressure of CO when the reaction has proceeded halfway, is used to represent the formation constants. The solubility coefficient of CO in CH_2Cl_2 was taken as 6.7×10^{-3} M/atm[53] and used to calculate the formation constant, K.

Collection of the X-ray Data and Structure Determination for the py adduct of 8a. Single crystals suitable for X-ray diffraction were obtained from $CHCl_3/CH_3OH$ plus a few drops of pyridine. Data were collected on a Nonius KappaCCD diffractometer at −100 °C using Mo−Kα graphite monochromated radiation (λ = 0.7107 Å), ϕ scans.

(52) Ellis, J.; Linard, P. E.; Szymanski, T.; Jones, R. D.; Budge, J. R.; Basolo, F. *J. Am. Chem. Soc.* **1980**, *102*, 1889−1896.
(53) Rougee, M.; Brault, D. *Biochemistry* **1975**, *14*, 4100−4106.

Scheme 1

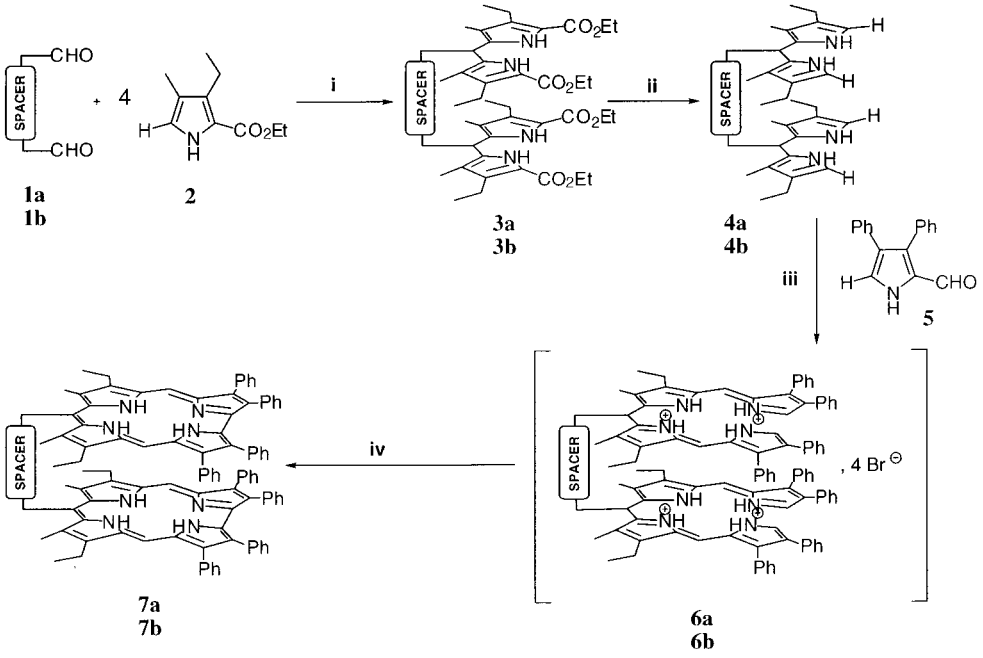

(i) : HCl, methanol, 3h, (85%); (ii) : KOH, $HO(CH_2)_2OH$, 190°C, 3h (90%); (iii) : HBr / CH_3CO_2H, 4h; (iv) : $NaHCO_3$, *p*-chloranil, N_2H_4 (50%).

The structure was solved using direct methods and refined against $|F|$. For all computations, the OpenMoleN package was used.[54]

Crystal Data for 8a (py)$_3$. Red crystals, crystal dimensions 0.20 × 0.20 × 0.15 mm^3: $C_{129}H_{101}Co_2Cl_6N_{11} = C_{127}H_{99}Co_2N_{11}\cdot 2CHCl_3$, M = 2135.90, triclinic, space group $P\bar{1}$, a = 13.2555(5) Å, b = 18.6406(8) Å, c = 22.2140(9) Å, α = 94.186(9)°, β = 102.273(9)°, γ = 94.205-(9)°, V = 5326.8(4) Å^3, Z = 2, D_c = 1.33 g cm^{-3}, μ(Mo−Kα) = 0.520 mm^{-1}. A total of 9293 independent reflections were collected, 2.5° < θ < 26.4°, 9075 reflections having $I > 3\sigma(I)$. One ethyl has its terminal methyl group disordered over two positions and also one of the two $CHCl_3$ molecules has the chlorines disordered over two positions. The hydrogen atoms were introduced as fixed contributors (d_{C-H} = 0.95 Å, $B_H = 1.3B_{equiv}(C)$ Å^2) with the exception of those of the disordered atoms. All non-hydrogen atoms, with the exception of the disordered atoms, were refined anisotropically. Final results $R(F)$ = 0.066, $R_w(F)$ = 0.084, GOF = 1.173, maximum residual electronic density 1.007 e Å^{-3}. Data for this structure have been deposited with the Cambridge Crystallographic Data Centre as Supplementary publication no. CCDC-168248.

Results and Discussion

Synthesis. The free base anthracenyl and biphenylenyl biscorroles **7a** and **7b** were synthesized in four steps starting from the corresponding diformyl spacer (Scheme 1).[48]

The condensation of 4 equiv of **2** on the diformyl spacer **1a** or **1b** under acidic conditions gave **3a** or **3b** in 80% yield (step i in Scheme 1). In a second step, **3a** or **3b** were simultaneously saponified and decarboxylated in diethylene glycol containing KOH at 190 °C to give **4a** or **4b** (step ii in Scheme 1). The free base cofacial biscorrole products, **7a** and **7b**, were obtained from condensation of 4 equiv of pyrrole **5** on **4a** or **4b** to give **6a** and **6b** (step iii in Scheme 1) which were not isolated and immediately cyclized by addition of sodium hydrogen carbonate.[55−58] The final macrocycle oxidation (step iv) was performed by adding a small amount of *p*-chloranil and the excess oxidant was reduced by addition of 50% hydrazine in water.[59] The progress of each step in this latter reaction was monitored by UV−visible spectroscopy.

meso-Aryl substituted corroles are generally unstable and decompose in the presence of air and light when left in solution.[60] One decomposition product has a biliverdin type structure which results from addition of dioxygen across the 1,19-double bond of the corrole ring.[60] The same instability is observed for linear biscorroles having methyl and ethyl substituents and a linear bisbiliverdin was isolated as a final product.[61] Bisbiliverdins are not found when phenyl groups are introduced at the β-pyrrole positions 2, 3, 17, and 18 of the corrole (see Chart 1 for numbering), and no ring opening occurs at the direct pyrrole−pyrrole 1,19-double bond.[60] The tetraphenyl free base corroles are quite stable in solution when in the dark but exhibit slow degradation of the macrocycle when left in the light over a period of several days. Results on a series of free base and Co(III) monocorroles with phenyl substituents at the β-positions show that the highest stability is obtained in the case of the Me_4Ph_5Cor derivative,[50] and this macrocycle was therefore used in synthesis of the two biscorroles $(BCA)H_6$ and $(BCB)H_6$.

The free base "face-to-face" biscorroles **7a** and **7b** were identified by LSIMS mass spectrometry which showed the

(54) *OpenMoleN, I. S. S.*; Nonius B. V.: Delft, The Netherlands, 1997.
(55) Genokhova, N. S.; Melent'eva, T. A.; Berezovskii, V. M. *Russ. Chem. Rev.* **1980**, *49*, 1056−1067.
(56) Dolphin, D.; Harris, R. L. N.; Huppatz, J. L.; Johnson, A. W.; Kay, I. T.; Leng, J. *J. Chem. Soc. C* **1966**, 98−106.
(57) Johnson, A. W.; Kay, I. T. *Proc. Chem. Soc.* **1964**, 89−90.
(58) Johnson, A. W.; Kay, I. T. *Proc. R. Soc. London A* **1965**, *288*, 334−341.
(59) Murakami, Y.; Matsuda, Y.; Sakata, K.; Yamada, S.; Tanaka, Y.; Aoyama, Y. *Bull. Chem. Soc. Jpn.* **1981**, *54*, 163−169.
(60) Tardieux, C.; Gros, C. P.; Guilard, R. *J. Heterocycl. Chem.* **1998**, *35*, 965−970.
(61) Paolesse, R.; Sagone, F.; Macagnano, A.; Boschi, T.; Prodi, L.; Montalti, M.; Zaccheroni, N.; Bolletta, F.; Smith, K. M. *J. Porphyrins Phthalocyanines* **1999**, 364−370.

Table 1. Selected Absorption Maxima (ϵ) of Representative Free Base Biscorroles and Bisporphyrins in CH_2Cl_2

		λ_{max}, nm ($\epsilon \times 10^3$ L mol^{-1} cm^{-1})					
macrocycle	compound	Soret band	Visible-bands				ref[a]
corrole	$(BCA)H_6$ (**7a**)	416 (131.5)			572 (35.4)	608 (29.0)	tw
	$(BCB)H_6$ (**7b**)	404 (141.0)			578 (44.5)	607 (37.0)	tw
	$(Me_4Ph_5Cor)H_3$	419 (85.0)			567 (15.0)	607 (13.0)	50
porphyrin	$(DPA)H_4$	395 (190.5)	506 (14.1)	539 (5.1)	578 (6.0)	631 (3.3)	21
	$(DPB)H_4$	379 (173.9)	511 (6.3)	540 (2.0)	580 (3.4)	632 (1.8)	21
	$(Me_6Et_2PhP)H_2$	404 (186.4)	501 (15.6)	535 (7.8)	570 (7.2)	623 (2.7)	64

[a] tw = this work.

pseudo-molecular ion $[M + H]^+$ (see Experimental Section). The UV−visible spectral data of these cofacial biscorroles are summarized in Table 1 and are not simply a superposition of absorption bands for the two corrole macrocycles. $(BCB)H_6$, **7b**, has a Soret band at 404 nm, and this can be compared to $(Me_4Ph_5Cor)H_3$ which possesses the same substitution pattern on the macrocycle but has a Soret band at 419 nm with about half the Soret band molar absorptivity as that of the biscorrole (see Table 1).

As in the case of the "Pacman" porphyrins,[21] the blue-shift of the Soret band upon going from the monocorrole, $(Me_4Ph_5Cor)H_3$, to the biscorrole **7b** can be explained by a strong electronic interaction between the two corrole rings which are held in close proximity to each other by the biphenylenyl spacer. This strong interaction between the two macrocycles leads to a higher HOMO−LUMO gap for **7b** than for the related monocorrole, and therefore the transitions occur at lower wavelengths for $(BCB)H_6$. This is also seen in the case of double decker porphyrins.[62,63]

For example, the Soret band of $(DPB)H_4$ in CH_2Cl_2 is located at 379 nm, while its monoporphyrin analogue, 13,17-diethyl-2,3,7,8,12,18-hexamethyl-5-phenylporphyrin, $(Me_6Et_2PhP)H_2$, has a Soret band at 404 nm.[64] This 25 nm difference is larger by 10 nm than the difference between the Soret bands of **7b** (404 nm) and the reference monocorrole, $(Me_4Ph_5Cor)H_3$ (419 nm, Table 1). Conversely, the distance between the two corrole rings in the anthracenyl derivative **7a** is probably large enough to avoid significant interaction between the two macrocycles, and, as a consequence, the optical spectrum of **7a** is characterized by absorption bands which are nearly identical in wavelength to those of the monocorrole $(Me_4Ph_5Cor)H_3$ (see Table 1). The difference in λ_{max} between the Soret bands of **7a** and $(Me_4Ph_5Cor)H_3$ is only 3 nm (see Table 1), and this is in contrast to what is seen for $(DPA)H_4$ and $(Me_6Et_2PhP)H_2$ where a 9 nm difference is observed between the Soret bands of the bisporphyrin and the related monoporphyrin with the same macrocycle substitution pattern. In the case of the cofacial biscorroles, **7a** and **7b**, a 12 nm difference is observed between the Soret band of the two compounds, and this can be compared to a difference of 16 nm between the Soret band of $(DPA)H_4$ and $(DPB)H_4$.

The ^{1}H NMR spectra of **7a** and **7b** exhibit the same ring current effects as seen in the Pacman porphyrin series.[24,65] Due to the close proximity of the two corrole rings to each other in **7b**, the NH signal of the free base macrocycles is shifted upfield ($\delta_{NH} = -5.49$ ppm) with respect to the two NH signals of the anthracenyl compound ($\delta_{NH} = -3.00$ and -2.83 ppm; see Experimental Section).

The upfield shift of the NH protons results from the superposition of the two ring currents of the corrole macrocycles which is enhanced in **7b**. The interaction of the two macrocycles is weaker in the case of **7a** than in the case of **7b**, and the NH signals therefore appear approximately in the same region as the reference $(Me_4Ph_5Cor)H_3$ monocorrole ($\delta_{NH} = -2.70$ ppm).[50]

UV−visible and NMR data suggest that **7a** can be considered as containing two separate monocorrole systems, but this is not the case for **7b** which exhibits a strong electronic interaction between the two macrocycles and can therefore be considered as a single unit containing the two corrole macrocycles. Interestingly, the two methylene protons of each β-pyrrole ethyl group in $(BCA)H_6$ and $(BCB)H_6$ are diastereotopic and two double quartets are seen at 3.27 and 3.22 ppm for $(BCA)H_6$ and a multiplet at 3.54 ppm for $(BCB)H_6$ (see Experimental Section). This results from a slow rotation of the ethyl groups of the biscorroles on the ^{1}H NMR time scale as is also the case for the Pacman porphyrins.

A standard procedure was employed to metalate the biscorroles **7a** and **7b** with cobalt.[48,66−68] The free base biscorroles were heated to 80 °C in pyridine containing excess cobalt(II) acetate,[69] and the progress of the metalation was monitored by UV−visible spectroscopy. Purification by column chromatography gave **8a** or **8b**, both of which, as shown in the following section, contain axially coordinated pyridine.

A noticeable color change from green to red was observed upon evaporating to dryness the pyridine solution. When redissolved in CH_2Cl_2, both cobalt complexes have well-defined Soret bands at 402 (**8a**) or 390 nm (**8b**) and a single Q-band at 527 (**8a**) or 521 nm (**8b**) (see Table 2). The spectrum of the pyridine complex could be recovered by adding pyridine to the previously evaporated compound, thus indicating a reversible coordination of one or more pyridine molecules at each metal center.

(62) Buchler, J. W.; Dennis, K. P. N. In *The Porphyrin Handbook*; Kadish, K. M., Smith, K. M., and Guilard, R., Eds.; Academic Press: San Diego, CA, 2000; Vol. 3, p 245.
(63) Kadish, K. M.; Moninot, G.; Hu, Y.; Dubois, D.; Ibnlfassi, A.; Barbe, J.-M.; Guilard, R. *J. Am. Chem. Soc.* **1993**, *115*, 8153−8166.
(64) Synthesis of 13, 17-diethyl-2,3,7,8,12,18-hexamethyl-5-phenylporphyrin. This compound was synthesized as described by Harris et al. (Harris, D.; Johnson, A. W.; Gaete-Holmes, R. *Bioorg. Chem.* **1980**, *9*, 63−70) by condensation of 1 equiv of the corresponding a, *c*-biladiene to 1 equiv of benzaldehyde. (Yield: 40%) ^{1}H NMR: δ 10.15 (s, 2H, meso), 9.94 (s, 1H, meso), 8.02 (d, 2H, Ph), 7.71−7.75 (d+s, 2H+1H, Ph), 4.06 (q, 4H, $-CH_2CH_3$), 3.62 (s, 6H, $-CH_3$), 3.52 (s, 6H, $-CH_3$), 2.44 (s, 6H, $-CH_3$), 1.87 (t, 6H, $-CH_2CH_3$), −3.02 (s, 1H, NH), −3.12 (s, 1H, NH). MS: $m/z = 523$ $[M]^{\cdot+}$. UV−vis (CH_2Cl_2; λ_{max}, nm (ϵ, L mol^{-1} cm^{-1})): 404 (186 400), 501 (15 600), 535 (7800), 570 (7200), 623 (2700). Anal. Calcd for $C_{36}H_{38}N_4$: C, 82.08; H, 7.28; N, 10.64. Found: C, 82.26; H, 7.59; N, 10.99.
(65) Chang, C. K. *J. Heterocycl. Chem.* **1977**, *14*, 1285−1288.
(66) Hitchcock, P. B.; McLaughlin, G. M. *J. Chem. Soc., Dalton Trans.* **1976**, 1927−1930.
(67) Paolesse, R.; Licoccia, S.; Fanciullo, M.; Morgante, E.; Boschi, T. *Inorg. Chim. Acta* **1993**, *203*, 107−114.
(68) Conlon, M.; Johnson, A. W.; Overend, W. R.; Rajapaksa, D. *J. Chem. Soc., Perkin Trans. 1* **1973**, 2281−2288.
(69) Murakami, Y.; Yamada, S.; Matsuda, Y.; Sakata, K. *Bull. Chem. Soc. Jpn.* **1978**, *51*, 123−129.

Table 2. Selected Absorption Maxima (%) of Representative Cobalt Biscorroles

compound	solvent[a]	λ_{max}, nm (%) Soret band	Visible bands			
$(BCA)Co_2$ (**8a**)	CH_2Cl_2	402 (100.0)	527 (28.3)			
	neat py	419 (96.3, sh[b]), 433 (100.0)	514 (15.2)	555 (25.7)	599 (62.8)	
$(BCB)Co_2$ (**8b**)	CH_2Cl_2	390 (100.0)	521 (39.0)			
	neat py	417 (100), 435 (95.2, sh[b])	517 (33.3)	556 (28.6)	603 (47.6)	
$(Me_4Ph_5Cor)Co$ [50]	CH_2Cl_2	398 (100)		529 (35.5)		
	neat py	412 (89.6, sh[b]), 433 (100.0)		557 (27.3)	598 (62.3)	616 (50.0, sh)

[a] py = pyridine. [b] sh = shoulder peak.

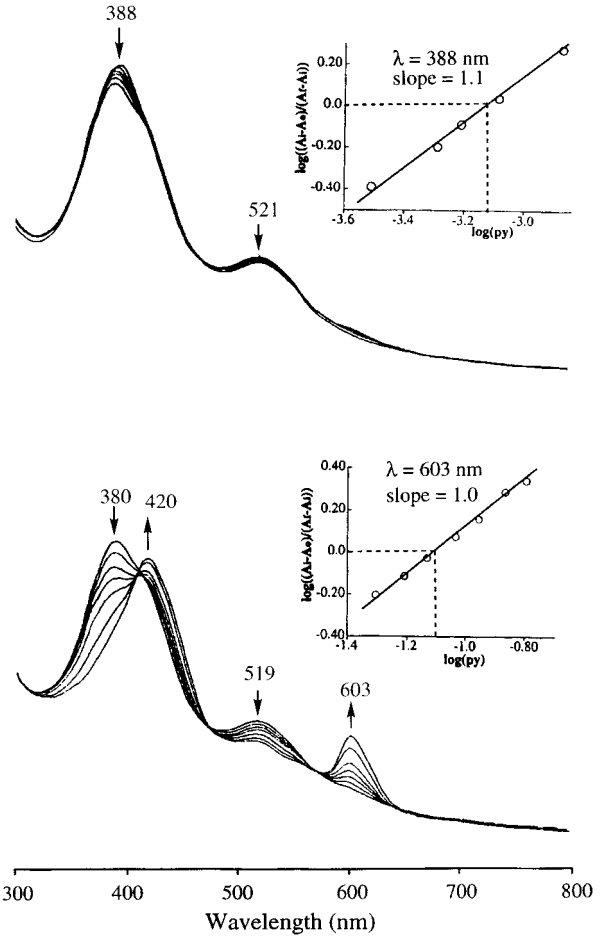

Figure 1. Electronic absorption spectral changes of 1.0×10^{-5} M **8b** upon (top) formation of $(BCB)Co_2(py)_2$ and (bottom) $(BCB)Co(py)_3$ in CH_2Cl_2. The inset of each figure shows the Hill plot for each pyridine addition. The pyridine concentration for the plots ranges (a) from 3.1×10^{-4} to 1.3×10^{-3} M and (b) from 5.2×10^{-2} to 0.16 M.

Ligand Binding Reactions of $(BCA)Co_2$ and $(BCB)Co_2$ with Pyridine and CO. The electronic absorption spectra of **8a** and **8b** were measured in CH_2Cl_2 during a titration with pyridine. The spectral changes obtained as the concentration of pyridine was varied from 10^{-4} to 10^{-3} M in a 1×10^{-5} M solution of $(BCB)Co_2$ are shown in Figure 1a. During the early stages of the titration, the broad Soret band centered at about 388 nm and the single visible band at 521 nm both slightly decrease in intensity. A Hill plot was constructed (see inset in Figure 1a) and shows a linear relationship with a slope of 1.1 and a binding constant of log $K_1 = 3.14$ for conversion of $(BCB)Co_2$ to $(BCB)Co_2(py)_2$ (eq 2). $(BCB)Co_2$ contains two equivalent cobalt centers, and the slope of ca. 1.0 indicates that each cobalt center binds one pyridine molecule.

$$(BCB)Co_2 + 2py \rightarrow (BCB)Co_2(py)_2 \qquad (2)$$

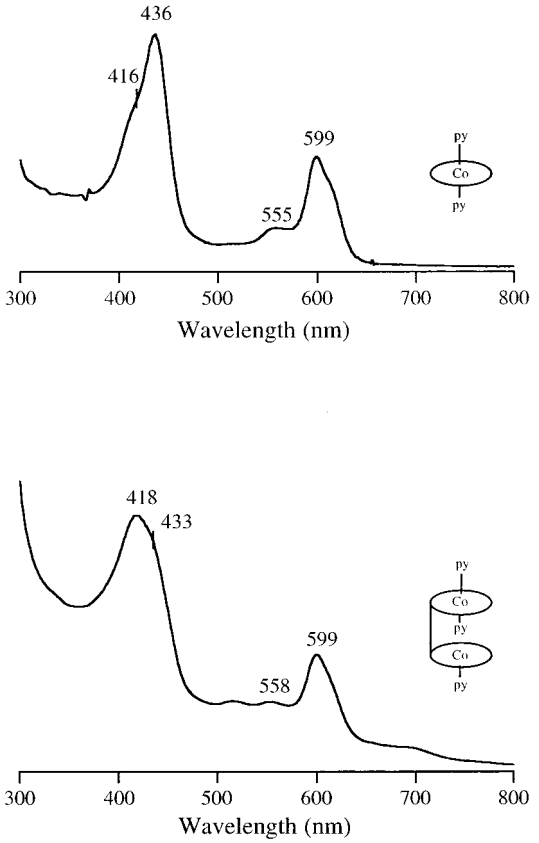

Figure 2. Electronic absorption spectra of (top) $(Me_4Ph_5Cor)Co$ in neat pyridine and (bottom) **8a** in CH_2Cl_2 containing 0.5 M pyridine.

The spectral changes of $(BCB)Co_2(py)_2$ as the pyridine concentration was increased from 10^{-3} to 0.2 M are illustrated in Figure 1b. As seen in the figure, the Soret band at 380 nm and the visible band at about 519 nm decrease simultaneously and this is accompanied by the appearance of a new Soret band at 420 nm and a new visible band at 603 nm. Another linear relationship with a slope of 1.0 is also obtained (inset of Figure 1b), and this ligand addition reaction is assigned to the conversion of $(BCB)Co_2(py)_2$ to $(BCB)Co_2(py)_3$ as shown in eq 3 ($\log K_2 = 1.10$).

$$(BCB)Co_2(py)_2 + py \rightarrow (BCB)Co_2(py)_3 \qquad (3)$$

Similar types of spectral changes are seen for $(BCA)Co_2$ in CH_2Cl_2, and the values of $\log K_1$ and $\log K_2$ are calculated as 4.84 and 2.61. These data are also interpreted in terms of $(BCA)Co_2(py)_2$ and $(BCA)Co_2(py)_3$ formation in mixed CH_2Cl_2/py solvents. The trispyridine adduct was structurally characterized in the case of $(BCA)Co_2$ (see following section).

Figure 2 compares the final spectrum in the pyridine titration of **8a** with the spectrum of $(Me_4Ph_5Cor)Co(py)_2$. The monocorrole bispyridine complex (Figure 2a) exhibits a Soret band

Table 3. Equilibrium Constants of Bis-Cobalt Corroles Binding Pyridine or CO in CH_2Cl_2 at 296 K

	pyridine		CO		
compound	log K_1[a]	log K_2[a]	$P_{1/2}^{CO}$ (Torr)	log K[b]	ν_{co} (cm^{-1})
$(Me_4Ph_5Cor)Co$	4.90	2.10	7.1	4.2	2049
$(BCA)Co_2$ (**8a**)	4.84	2.61	15.0	3.9	2047
$(BCB)Co_2$ (**8b**)	3.14	1.10	31.3	3.6	2046

[a] K_1 corresponds to eq 2 and K_2 to eq 3. [b] $K = (P_{1/2}^{CO}k_H)^{-1}$; $k_H = 6.7 \times 10^{-3}$ M/atm in CH_2Cl_2.

at 436 nm, a shoulder at ca. 416 nm, and two visible bands at 555 and 599 nm. The intensity of the visible band at 599 nm is much stronger than that of the second visible band at 555 nm. A split Soret band (at 418 and 433 nm) and two visible bands (at 558 and 599 nm) are also observed in the final spectrum of titrated **8a** (Figure 2b), but the intensity of the band at 418 nm is stronger than that at 433 nm which appears as a shoulder of the major peak. This difference in spectral properties between the monocorrole and the biscorrole suggests that more than one pyridine molecule may be bound within the cavity of $(BCA)Co_2$ at very high pyridine concentrations. Therefore, the spectrum in Figure 2b could be assigned to a mixture of overlapping spectra for five- and six-coordinate cobalt corrole complexes, i.e., $(BCA)Co_2(py)_3$ and $(BCA)Co_2(py)_4$.

The pyridine binding constants of $(BCA)Co_2$ and $(BCB)Co_2$ are summarized in Table 3, where K_1 is defined by eq 2 and K_2 by eq 3. Comparison of formation constants for the two biscorroles with those of the corresponding monocorrole complex shows that log K_1 for **8a** is only a slightly smaller than log K_1 for the addition of py to $(Me_4Ph_5Cor)Co$. However, a much smaller log K_1 is seen for **8b** as compared to the other two compounds.

The titration of **8a** and **8b** with CO in CH_2Cl_2 was monitored by measuring changes in the UV−visible spectra as a function of CO partial pressure, and these results are illustrated in Figure 3 for the case of $(BCB)Co_2$. The starting compound has a broad Soret band at ca. 388 nm and a visible band at 521 nm. As CO is introduced into solution, the intensity of the Soret band decreases and a new visible band appears at 569 nm. No other spectral changes are seen as the CO partial pressure is increased up to 1 atm. The Hill plot (inset of Figure 3) shows a linear relationship, and a slope of 1.0 is obtained. A comparison of spectral changes for **8b** upon CO binding with results for CO binding to the corresponding monocorrole, $(Me_4Ph_5Cor)Co$,[50] clearly indicates that each cobalt unit in the biscorrole binds a single CO molecule as schematically shown in eq 4.

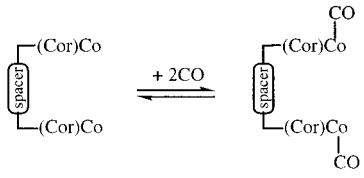

(4)

The CO partial pressure when the binding reaction has proceeded halfway, is obtained from the Hill equation, and the experimentally obtained value of $P_{1/2}^{CO} = 31.3$ Torr for **8b** corresponds to a log $K = 3.6$. The value of $P_{1/2}^{CO}$ is 15.0 Torr for **8a**, and log $K = 3.9$. The CO binding ability of **8b** is less than that of $(BCA)Co_2$ or $(Me_4Ph_5Cor)Co$, and this trend is also seen in the pyridine binding constants (Table 3).

The CO stretching frequencies of both biscorrole complexes were also measured in CH_2Cl_2 under a CO atmosphere (Table 3). The ν_{CO} are located at 2047 cm^{-1} for **8a** and 2046 cm^{-1} for **8b**, both of which are slightly lower than the ν_{CO} of the monocorrole $(Me_4Ph_5Cor)Co$ whose Co−CO stretch is located at 2049 cm^{-1}.

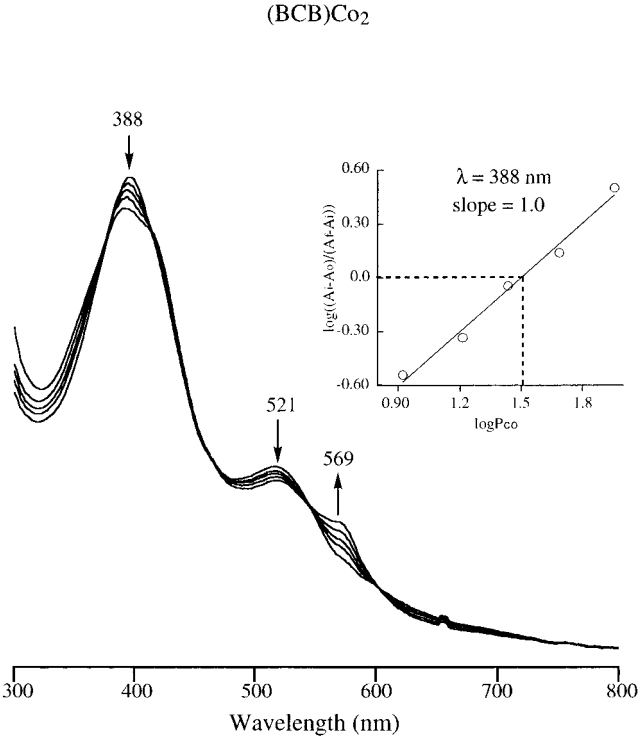

Figure 3. Electronic absorption spectral changes upon formation of $(BCB)Co_2(CO)_2$ from 1.5×10^{-5} M $(BCB)Co_2$. The Hill plot for the CO binding reaction is shown as an inset where the CO partial pressure ranges from 16 to 600 Torr for the plot.

Molecular Structure of $(BCA)Co_2(py)_3$. Side and front views of the molecular structure of $(BCA)Co_2(py)_3$ are displayed in Figure 4a,b, respectively. This figure also gives the labeling scheme used for most of the non-hydrogen atoms. Crystal data for $(BCA)Co_2(py)_3 \cdot 2CHCl_3$ and details of the diffraction data are listed in Table 4, and selected bond distances are summarized in Table 5.

$(BCA)Co_2(py)_3$ is a homobimetallic complex of a face-to-face biscorrole. The six-coordinate cobalt(III) cation, Co1, is bound to the four pyrrole nitrogen atoms N21 to N24 of the corrole ring Cor1 and also to the nitrogen atoms N45 and N51 of the two axially coordinated pyridine molecules Py1 and Py2. Py2 lies in the cavity formed by both corrole rings of the face-to-face biscorrole molecule, whereas Py1 lies outside this cavity. In contrast to Co1, the second cobalt atom, Co2 is five-coordinate, bound to the four pyrrole nitrogen atoms N41 to N44 of the corrole ring Cor2 and to the nitrogen atom N131 of the single pyridine Py3, located as the Py1 molecule outside of the molecular cavity. Thus, the coordination polyhedra of the two cobalt atoms Co1 and Co2 of $(BCA)Co_2(py)_3$ are octahedral and square-pyramidal, respectively.

The Co1−Np and Co2−Np (Np: pyrrole nitrogen atom) bond distances are not significantly different, their mean value being 1.887(5) Å. Again, the shortest Co−Np bond distances (Co1−N21 = 1.879(4), Co1−N24 = 1.883(5), and Co2−N41 = 1.875(5) Å) correspond in each case to cobalt−pyrrole nitrogen bonds involving two Nps belonging to the pyrrole rings linked directly via the C_α–C_α bond. Similar features have been previously observed in the structures of the cobalt corrole complex, $(Me_4Ph_5Cor)Co(py)_2$[50] and other metallocorroles.[29,30] The average Co−Np bond distance of 1.887(5) Å found in $(BCA)Co_2(py)_3$ is not significantly different from the 1.899(6) Å seen in $(Me_4Ph_5Cor)Co(py)_2$, a compound in which the cobalt(III) ion is six-

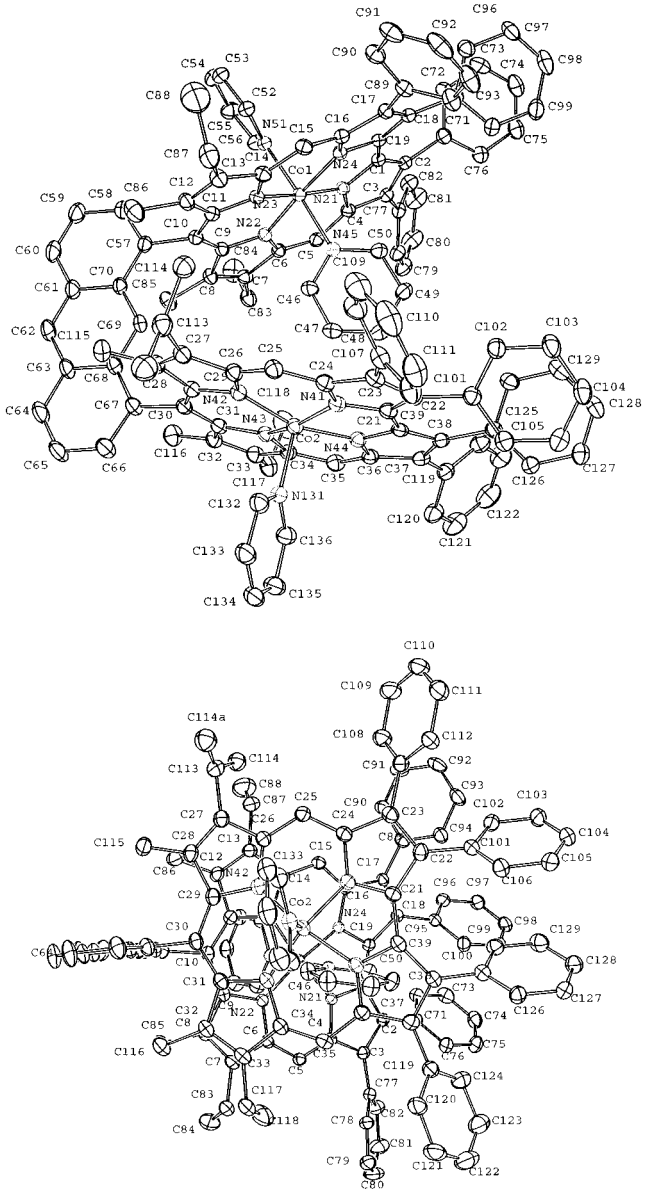

Figure 4. (top) Side and (bottom) front views of the molecular structure and atom numbering of $(BCA)Co_2(py)_3$. Thermal ellipsoids enclose 30% probability. Hydrogen atoms are omitted for clarity.

coordinate and low-spin. The similarity of Co−Np bond distances betweenCo1 and Co2 in $(BCA)Co_2(py)_3$ and the cobalt atom in $(Me_4Ph_5Cor)Co(py)_2$ suggests that both cobalt(III) atoms in $(BCA)Co_2(py)_3$, the six-coordinate Co1, and the five-coordinate Co2, are each low-spin. The Co−Npy axial bond distances are very similar to each other, although the Co2−N131 bond distance of 1.946(5) Å, with the five-coordinate cobalt Co2, is slightly shorter than the Co1−Npy bond lengths of 1.976(5) (Co1−N45) and 1.979(5) Å (Co1−N51) involving the six-coordinate cobalt atom, Co1. These Co−Npy bonds are slightly tilted away from the two lines perpendicular to the corrole mean planes going through each cobalt atom, the corresponding angles being 5.2(2) (Co1−N51), 3.3(2) (Co1−N45), and 2.9(2)° (Co2−N131). Moreover, the orientation of the pyridine rings Py1 and Py2 around Co1 is almost staggered, the dihedral angle between the mean planes of the two pyridine rings being 88.3(2)°.

The Co−Np and axial Co−Npy bond distances in $(BCA)Co_2(py)_3$ are significantly shorter than the corresponding distances in the low-spin, six-coordinate cobalt(III) porphyrin, $[(TPP)Co(pip)_2]^+$, where the average Co−Np and Co−N(pip) bond distances are 1.979 and 2.060 Å, respectively.[70] As in $(Me_4Ph_5Cor)Co(py)_2$,[50] the shortening of the Co−Np bond lengths in $(BCA)Co_2(py)_3$ can be ascribed to the reduced hole size of the two corrole rings occurring in $[BCA]^{6-}$ relative to the tetraphenylporphyrin ligand $[TPP]^{2-}$, since a similar decrease of the M−Np bond lengths was also observed in several other metallocorroles as different as $(Me_8Cor)Rh(AsPh_3)$,[71] $(Me_8Ph_3Cor)CoPPh_3$,[72] and $(Me_2Et_6Cor)Mn$.[73]

Both corrole rings, Cor1 and Cor2, of $(BCA)Co_2(py)_3$ are slightly ruffled as indicated by the displacements of the *meso* carbon atoms above and below the corrole-core mean plane. For the Cor1 ring, the *meso* carbon C10 lies 0.023(1) Å above the plane, whereas C5 and C15 lie on the average 0.019(1) Å

(70) Scheidt, W. R.; Cunningham, J. A.; Hoard, J. L. *J. Am. Chem. Soc.* **1973**, *95*, 8289−8294.
(71) Boschi, T.; Licoccia, S.; Paolesse, R.; Tagliatesta, P.; Azarnia Tehran, M.; Pelizzi, G.; Vitali, F. *J. Chem. Soc., Dalton Trans.* **1990**, 463−468.
(72) Paolesse, R.; Licoccia, S.; Bandoli, G.; Dolmella, A.; Boschi, T. *Inorg. Chem.* **1994**, *33*, 1171−1176.
(73) Licoccia, S.; Morgante, E.; Paolesse, R.; Polizio, F.; Senge, M. O.; Tondello, E.; Boschi, T. *Inorg. Chem.* **1997**, *36*, 1564−1570.

Table 4. X-ray Experimental Data for Compound **8a**

formula	$C_{129}H_{101}Cl_6Co_2N_{11}$-$C_{127}H_{99}Co_2N_{11}\cdot 2CHCl_3$
MW	2135.90
cryst syst	triclinic
space group	$P\bar{1}$
a (Å)	13.2555(5)
b (Å)	18.6406(8)
c (Å)	22.2140(9)
α (deg)	94.186(9)
β (deg)	102.273(9)
γ (deg)	94.205(9)
V (Å^3)	5326.8(4)
Z	2
color	red
crystl dimens (mm)	0.20 × 0.20 × 0.15
D_{calc} (g cm^3)	1.33
F(000)	2216
μ (mm^{-1})	0.520
temp (K)	173
wavelength (Å)	0.71073
radiation	Mo Kα graphite monochromated
diffractometer	KappaCCD
scan mode	ϕ scans
hkl limits	0,16/−22,22/−27,27
Θ limits (deg)	2.5/26.39
no. of data with $I > 3\sigma(I)$	9075
no. of variables	1321
R	0.066
R_w	0.084
GOF	1.173
largest peak in final (e Å^3)	1.007

Table 5. Selected Bond Distances, Angles, and Averages for Compound **8a**

Co1−N21	1.879(4)	Co1−N45	1.976(5)
Co1−N22	1.898(5)	Co1−N51	1.979(5)
Co1−N23	1.905(4)		
Co1−N24	1.883(5)	Co2−N131	1.946(5)
<Co1−Np>	1.891(2)	<Co1−Npyridine>	1.978(3)
Co2−N41	1.875(5)	<Np−Cα>	1.379(6)
Co2−N42	1.884(4)	<Cα−Cβ>	1.442(6)
Co2−N43	1.880(5)	<Cβ−Cβ>	1.378(8)
Co2−N44	1.894(4)	<Cα−Cα′>	1.432(1)
<Co2−Np>	1.883(2)	<Cm−Cα>	1.392(6)
<Cα−Np−Cα>	108.7(6)	<Np−Cα−Cα′>	110.9(8)
<Np−Cα−Cβ>	108.2(4)	<Np−Cα−Cm>	122.8(9)
<Cα−Cβ−Cβ>	107.4(5)	<Cα−Cm−Cα>	125.1(4)

below this mean plane. The corrole ring Cor2 is even less ruffled, and C30 lies in the mean plane, whereas C25 and C35 are on the average displaced only by 0.09(1) Å above the corrole mean plane.

Co1 is not significantly displaced from the 4Np mean plane of Cor1. Its displacement relative to the Cor1-core mean plane is also very small (0.009(1) Å), and no doming is displayed by the Cor1 macrocycle. Five-coordinate Co2 lies 0.328(1) Å away from the mean plane of Cor2 and is displaced in the same direction by 0.252(1) Å from its 4Np mean plane. Thus, the separation between these mean planes is 0.076(1) Å, and, due to the five-coordination of Co2, the ring Cor2 is slightly domed.

As in the nickel(II) bisoxocorrole derivative, (BOCA)Ni_2,[74] the two corrole rings Cor1 and Cor2 are held together by a rigid and planar anthracenyl spacer group. However, due to steric

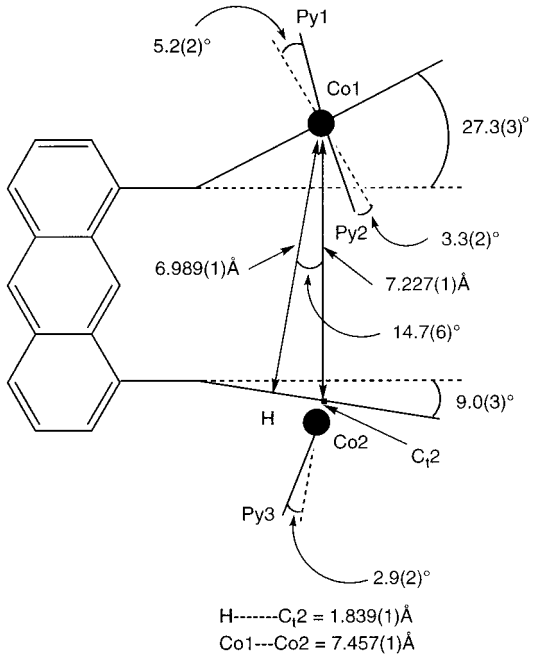

Figure 5. Orientation and position of the corrole ring mean planes relative to the anthracenyl spacer.

interactions between the atoms of Cor2 and the pyridine molecule Py2 which is axially bonded to Co1, the two rings Cor1 and Cor2 are not stacked over one another but are displaced in opposite directions, as seen in Figure 5. For each ring, Cor1 and Cor2, the projection on a plane perpendicular to the mean plane of the anthracenyl spacer of the two lines connecting the *meso*-carbon opposite to the C_α–C_α bond with the middle of this bond (C10···C1/C19 and C30···C21/C39 is 10(1)°). The dihedral angles between the mean-planes of the two corrole rings Cor1 and Cor2 relative to the plane which is perpendicular to the mean plane of the anthracenyl spacer are 5.9(1)° for Cor1 and 3.7(1)° for Cor2. This orientation leads to an overall dihedral angle between the mean planes of Cor1 and Cor2 of 36.3(1)° and a lateral shift of 1.839(1) Å between C_t2, the center of the four pyrrole nitrogens lying in the 4Np mean plane of ring Cor2, and the projection, H, of Co1 on the mean plane of the corrole ring, Cor2 (Figure 5). The corresponding Co1−C_t2, Co1−Co2, and Co1−H distances are 7.227(1), 7.457(1), and 6.989(1) Å, the slip angle being 14.7(3)°. Short contact distances of 3.47, 3.50, and 3.54 occur between the carbon atoms C47 and C48 of Py2 and the pyrrole nitrogen N44. Other short contacts ranging from 3.64 to 3.75 occur between C47 and C48 and the carbon atoms C34, C35, C36, C37, C38, and C39 of Cor2.

The anthracenyl spacer is almost planar, the largest deviation from its mean plane is 0.070(7) Å (C66), and the mean-deviation is 0.035(7) Å. Two molecules are packed together in a head to tail manner around the inversion centers of space group $P\bar{1}$. The corresponding shortest intermolecular contacts occur between two Py1 pyridines of two molecules assembled in this way. The corresponding distances range from 3.41(1) to 3.95(1) Å. One of the two chloroform solvation molecules lies in the molecular cavity and is surrounded by phenyl groups and Py2 of different molecules. Two of its chlorine atoms are in contact with the carbon atoms C89, C93, C94, C102, C108, C117, and C123 of different phenyl groups and with C49 of Py2. The corresponding distances range from 3.689 to 3.987(1) Å. The second chloroform molecule in (BCA)$Co_2(py)_3\cdot 2CHCl_3$ lies in a cleft of the structure and is disordered.

(74) Jérôme, F.; Barbe, J. M.; Gros, C. P.; Guilard, R.; Fischer, J.; Weiss, R. *New J. Chem.* **2001**, *25*, 93−101.
(75) Kadish, K. M.; Adamian, V. A.; Van Caemelbecke, E.; Gueletii, E.; Will, S.; Erben, C.; Vogel, E. *J. Am. Chem. Soc.* **1998**, *120*, 11986−11993.

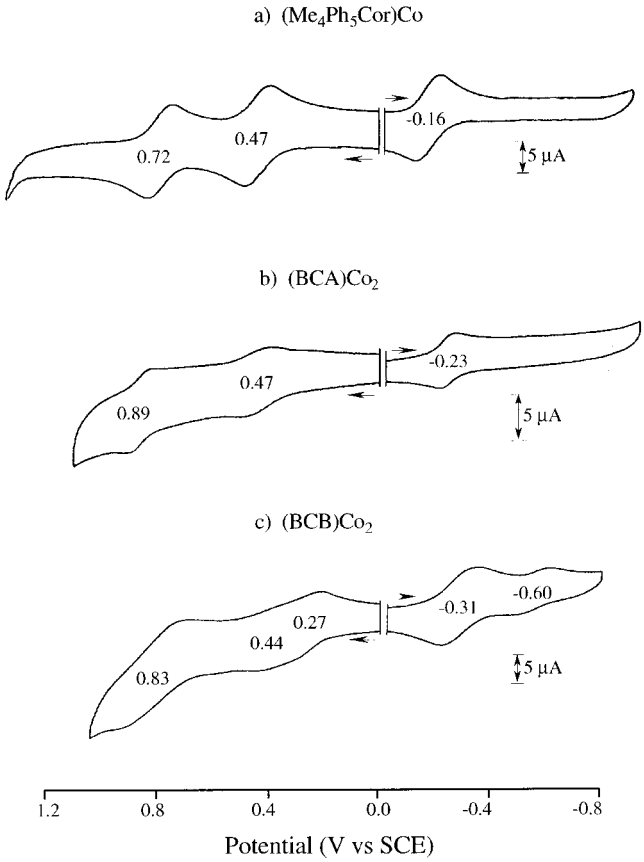

Figure 6. Cyclic voltammograms of 1.5×10^{-3} M $(Me_4Ph_5Cor)Co$, 3.0×10^{-3} M **8a,** and **8b** in PhCN, 0.2 M TBAP. Scan rate: 0.1 V/s.

Table 6. Half-Wave Potentials[a] in PhCN Containing 0.2 M TBAP for Corroles and 0.2 M $TBAPF_6$ for Porphyrins

	ox.			red.		
compound	third	second	first	first	second	ref[c]
$(Me_4Ph_5Cor)Co$		0.72	0.47	−0.16		50
$(BCA)Co_2$ (**8a**)		0.89	0.47	−0.23		tw
$(BCB)Co_2$ (**8b**)	0.83	0.44	0.27	−0.31	−0.60	tw
(MPA)Co			−0.06[b]	−1.53		77
$(DPA)Co_2$			0.05	−1.60		77
$(DPB)Co_2$		0.17	0.00	−1.71	−1.90	77

[a] V vs SCE for corrole complexes and V vs Fc/Fc^+ for porphyrin complexes. [b] E_{pa}, scan rate = 0.1 V/s. [c] *tw* = this work.

Electrochemistry of $(BCA)Co_2$ (8a) and $(BCB)Co_2$ (8b). The electrochemistry of **8a** and **8b** was examined in PhCN containing 0.2 M TBAP. The cyclic voltammograms are shown in Figure 6, which also includes that for $(Me_4Ph_5Cor)Co$,[50] and the redox potentials of each process are listed in Table 6. Two reversible to quasi-reversible oxidations are observed for **8a**, and the corresponding half-wave potentials are located at 0.47 and 0.89 V, respectively. Both $E_{1/2}$ values are comparable to those of the monocorrole complex, $(Me_4Ph_5Cor)Co$, with $E_{1/2} = 0.47$ and 0.72 V (see Figure 6 and Table 6). $(BCB)Co_2$, however, undergoes three reversible to quasi-reversible oxidations with half-wave potentials locating at 0.27, 0.44, and 0.83 V at a scan rate of 0.1 V/s. The first two oxidations represent two overlapped electrochemical processes with a 170 mV separation in $E_{1/2}$ as compared with that of $(Me_4Ph_5Cor)Co$ (Table 6). These two processes correspond to the stepwise one-electron abstraction from each macrocycle, leading to the formation of the cation radical and dication species. In contrast to this result, the first oxidation of **8a** shows only one reversible process.

$(BCA)Co_2$ undergoes a single Co(III)/Co(II) process at −0.23 V, while $(BCB)Co_2$ is reduced in two steps at $E_{1/2} = -0.31$ and −0.60 V. These two reductions are assigned to a stepwise one-electron addition to the cobalt centers.

The electrochemistry of several face-to-face cobalt bisporphyrins has been investigated.[4,23,25−28,76−80] Among the bisporphyrin complexes, the Pacman derivatives $(DPA)Co_2$ and $(DPB)Co_2$ have structures most similar to the two biscorrole complexes investigated in this present paper. Previous studies[77] have shown that $(DPA)Co_2$ and $(DPB)Co_2$ exhibit different electrochemical behavior due to a different distance between the porphyrin rings, and this is also the case for the two biscorroles (see Table 6). The two porphyrin units in $(DPA)Co_2$ can be oxidized or reduced simultaneously at the same or at very close potentials to each other. This distance between the two porphyrins is much larger in this compound than in $(DPB)Co_2$,[8,17] thus leading to a weaker $\pi-\pi$ electronic interaction between the two porphyrin units. This differs from $(DPB)Co_2$ where the first oxidation and the first reduction are split into two discrete one-electron steps indicating a significant interaction between the two redox active centers. Each porphyrin unit in the $(DPB)Co_2$ complexes is oxidized or reduced at a different potential. A similar result is seen for the two biscorrole complexes where $(BCB)Co_2$ undergoes two one-electron oxidations and two split one-electron reductions.

Acknowledgment. The support of the Robert A. Welch Foundation (K.M.K., Grant E-680) is gratefully acknowledged. This work was supported by the French Ministry of Research (MENRT) and CNRS (UMR 5633). These are gratefully thanked for financial support. The "Région Bourgogne" and "Air Liquide" company are acknowledged for a scholarship (F.J.). The authors are also grateful to M. Soustelle for the synthesis of pyrrole and dipyrromethane precursors.

Supporting Information Available: Crystallographic data for $(BCA)Co_2(py)_3$. This material is available free of charge via the Internet at http://pubs.acs.org.

IC0101782

(76) Le Mest, Y.; L'Her, M.; Courtot-Coupez, J.; Collman, J. P.; Evitt, E. R.; Bencosme, C. S. *J. Electroanal. Chem.* **1985**, *184*, 331−346.
(77) Le Mest, Y.; L'Her, M. *J. Electroanal. Chem.* **1987**, *234*, 277−295.
(78) Le Mest, Y.; L'Her, M.; Hendricks, N. H.; Kim, K.; Collman, J. P. *Inorg. Chem.* **1992**, *31*, 835−847.
(79) Ngameni, E.; Le Mest, Y.; L'Her, M.; Collman, J. P.; Hendricks, N. H.; Kim, K. *J. Electroanal. Chem.* **1987**, *220*, 247−257.
(80) Ngameni, E.; Laouénan, A.; L'Her, M.; Hinnen, C.; Hendricks, N. H.; Collman, J. P. *J. Electroanal. Chem.* **1991**, *301*, 207−226.